Science Signaling
AAAS

stke.sciencemag.org/cgi/content/full/12/598/eaaw3657/DC1

Supplementary Materials for

Kinetics of CXCL12 binding to atypical chemokine receptor 3 reveal a role for the receptor N terminus in chemokine binding

Martin Gustavsson, Douglas P. Dyer, Chunxia Zhao, Tracy M. Handel*

*Corresponding author. Email: thandel@ucsd.edu

Published 10 September 2019, *Sci. Signal.* **12**, eaaw3657 (2019)
DOI: 10.1126/scisignal.aaw3657

This PDF file includes:

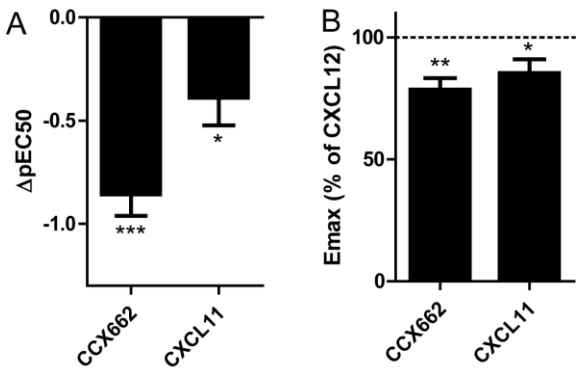

Fig. S1. β-Arrestin recruitment to ACKR3$_{WT}$ induced by CCX662 and CXCL11 in BRET experiments. (**A**) Potency of activation relative to CXCL12 was calculated from ΔpEC_{50}= $pEC_{50,CXCL12}$-$pEC_{50,CCX662/CXCL11}$. (**B**) Efficacy of CCX662 and CXCL11 normalized to CXCL12. Bars show the average and standard errors from five independent experiments. Significant differences for CCX662 and CXCL11 compared to CXCL12 are noted: *P<0.05, **P<0.01, ***P<0.001 from one-way ANOVA with Dunnett's multiple comparison test.

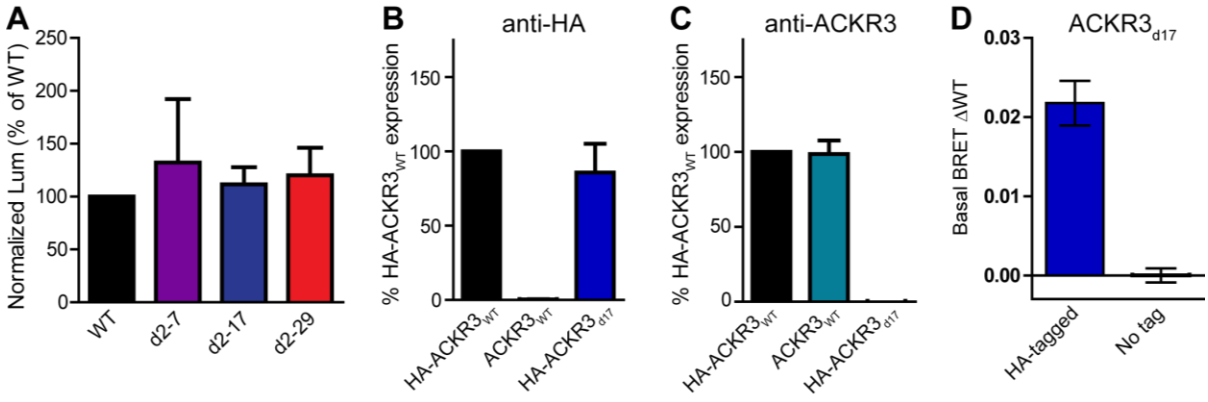

Fig. S2. Expression of ACKR3 variants in HEK cells. (**A**) Total expression in HEK293T cells determined by luminescence. Data were normalized to ACKR3$_{WT}$ expression from the same experiment according to Lum_{mutant}/Lum_{WT} x 100. (**B**) Surface expression of ACKR3 in HEK293T cells quantified from anti-HA antibody staining. (**C**) Same samples as in (A) stained with an anti-ACKR3 antibody. Surface expression of ACKR3$_{d17}$ is not detectable with the anti-ACKR3 antibody since the truncation removes the epitope for antibody binding. (**D**) Constitutive association of GFP10-β-arrestin-2 in HEK293T cells to Rluc-fused receptors. Data in are means ± SEM of three or more experiments.

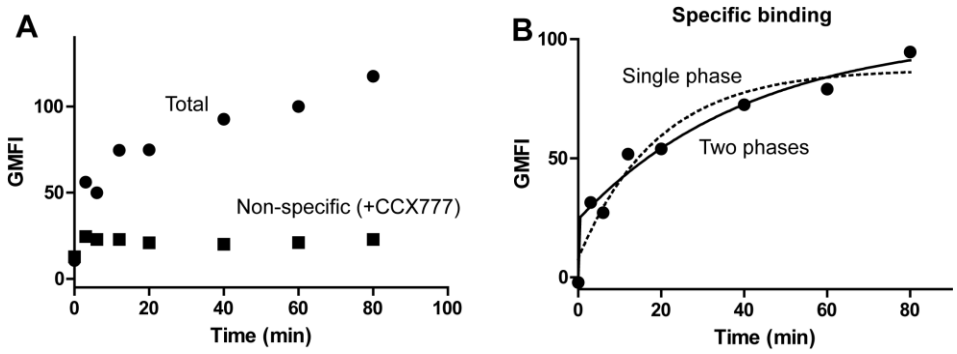

Fig. S3. Kinetics of association of CXCL12 with ACKR3 on live *Sf9* cells. (**A**) Representative example of association curve in the absence (total binding) and presence (non-specific binding) of the small molecule agonist CCX777 determined from the geometric mean fluorescent intensity (GMFI) of FITC-conjugated anti-HA antibody bound to CXCL12-HA. (**B**) Specific binding obtained by subtracting non-specific from total binding in (A). The fit of the association data is significantly improved with the use of a two-phase exponential function (solid line) compared to a single-phase exponential (dotted line). Data are representative of five experiments.

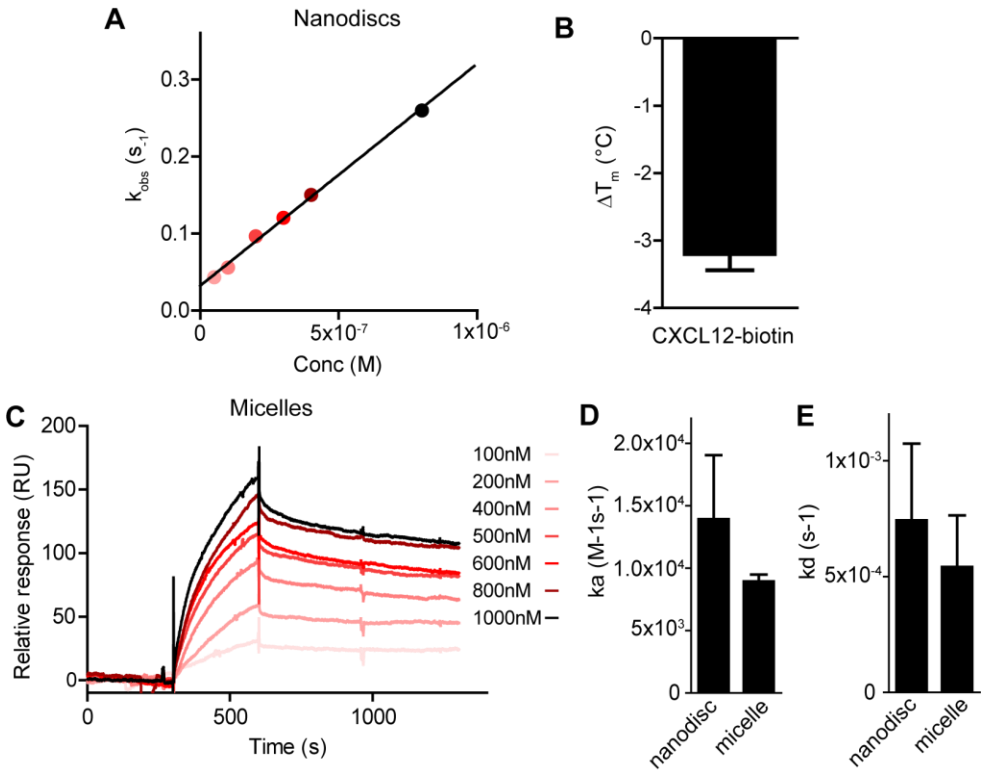

Fig. S4. SPR in nanodiscs and detergent micelles. (**A**) Analysis of CXCL12 binding for ACKR3 in nanodiscs. Plot of k_{obs} determined from fitting the association phase of the SPR curves at different concentrations of chemokine using a shared value for the dissociation rate constant (k_d). Linear regression indicates that the data fits to a straight line with a correlation coefficient (R^2) of 0.997. (**B**) Thermostability of ACKR3 in complex with biotinylated CXCL12 determined from CPM assays. ΔT_m was determined as $T_{m,ACKR3:CXCL12\text{-}biotin}$- $T_{m,ACKR3:CXCL12}$. Bars show the average and standard error of three measurements. (**C**) SPR curves for the binding of ACKR3 in DDM/CHS detergent micelles to immobilized CXCL12-biotin at different concentrations of receptor. (**D** and **E**) Association (k_a) and dissociation (k_d) constants determined from fitting SPR data in micelles and nanodiscs from three separate experiments.

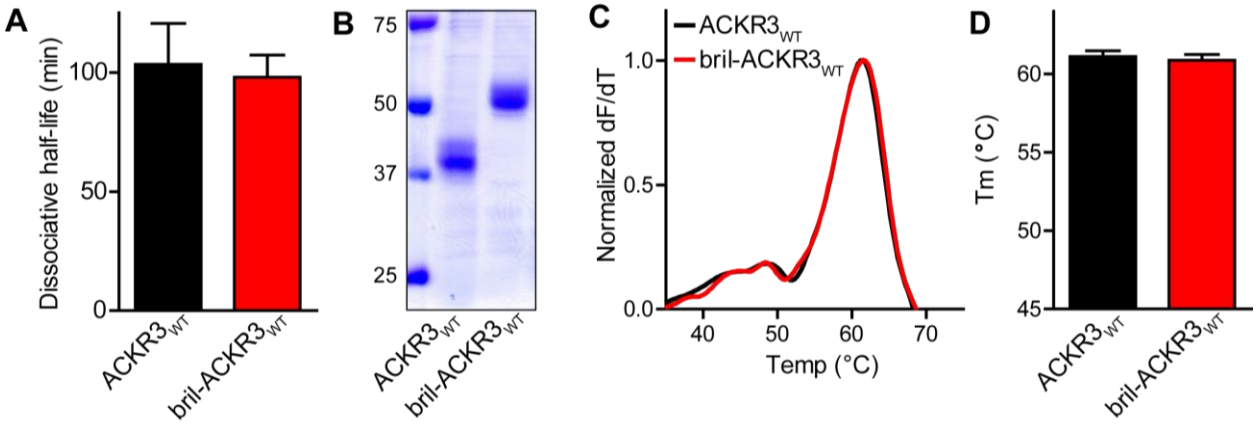

Fig. S5. N-terminal cytochrome b562-RIL fusion protein did not affect CXCL12 dissociation rate or folding of ACKR3. (**A**) Dissociative half-life for CXCL12 with $ACKR3_{WT}$ and bril-$ACKR3_{WT}$ in live *Sf9* cells. Bars correspond to averages and standard errors from n=4 ($ACKR3_{WT}$) or n=8 (bril-$ACKR3_{WT}$). (**B**) SDS-PAGE of $ACKR3_{WT}$ and bril-$ACKR3_{WT}$ purified from *Sf9* cells. (**C**) Thermostability of purified $ACKR3_{WT}$:$CXCL12_{WT}$ and bril-$ACKR3_{WT}$:$CXCL12_{WT}$ in detergent micelles measured by CPM fluorescence. Peaks at 61°C correspond to the midpoints of unfolding (Tm) values. (**D**) Mean and standard errors of three T_m measurements for $ACKR3_{WT}$ and bril-$ACKR3_{WT}$.

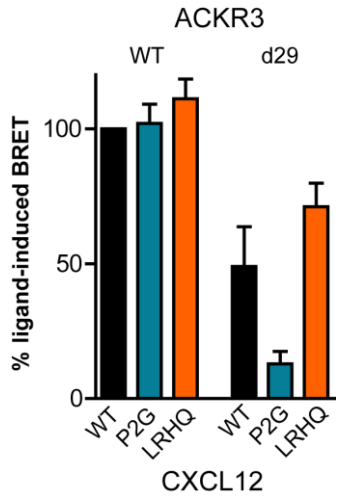

Fig. S6. BRET signal increase after addition of 2 µM chemokine for $ACKR3_{WT}$ and $ACKR3_{d29}$. % ligand-induced BRET was calculated as a percentage of CXCL12-induced BRET with $ACKR3_{WT}$ according to ($BRET_{2uM\ ligand}$-$BRET_{no\ ligand}$)/ ($BRET_{ACKR3\text{-}WT,2uM\ CXCL12}$-$BRET_{ACKR3\text{-}WTno\ ligand}$) x 100. Data are means ± SEM of three experiments.

Table S1. IC_{50} values (nM) for equilibrium binding studies reported in literature. Ref, reference; first author listed.

	Ref	Author	CXCR4	ACKR3
1	(33)	Hanes	2.1	0.0014
2	(47)	Hoffmann	23.8	2.6
3	(35)	Szpakowska	12.9	1.8
4	(38)	Montpas		5.9
5	(34)	Benredjem		3.0
6	(48)	Wijtmans		0.63
7	(49)	Canals		0.2
8	(50)	Zabel		0.2
9	(50)	Zabel		0.07
10	(50)	Zabel		0.1
11	(4)	Burns		0.2
12	(5)	Rajagopal		0.2
13	(51)	Balabanian		0.8
		Average 1-3:	12.9	1.47
		Average all:		1.21